

Contents lists available at UGC-CARE

## International Journal of Pharmaceutical Sciences and Drug Research

[ISSN: 0975-248X; CODEN (USA): IJPSPP]

Available online at www.ijpsdronline.com



**Research Article** 

# Quality-by-Design Optimization of Electrospinning Parameters to Formulate Scaffolds for Topical Inflammatory Disease Management *via* Drug Repurposing

Alka\*, Shubhini A Saraf

Department of Pharmaceutical Sciences, Babasaheb Bhimrao Ambedkar University (A Central University), Lucknow, Uttar Pradesh, India

#### ARTICLE INFO

#### **Article history:**

Received: 26 January, 2024 Revised: 16 March, 2024 Accepted: 19 March, 2024 Published: 30 March, 2024

#### **Keywords:**

Electrospinning, CS/PVA polyblend nanofiber scaffolds, Experimental design, Surface morphology.

#### DOI:

10.25004/IJPSDR.2024.160214

#### ABSTRACT

This study investigates the fabrication of chitosan (CS)/polyvinyl alcohol (PVA) blend nanofibers *via* electrospinning, aiming to create nanofibers with enhanced properties for broad applications. The research focuses on optimizing electrospinning parameters to reduce bead formation and achieve uniform nanofiber morphology. A detailed experimental design, employing a nineteen-point plan developed with Design-Expert software, examined variables such as polymer concentration, distance from the needle to the collector, the required voltage, and the rate at which solution was ejected from the needle. Morphological characteristics of the nanofibers were analyzed using advanced microscopy, complemented by drug release and wound healing assessments. The optimal electrospinning conditions were determined to be a 1:3 CS/PVA solution concentration ratio, an 8 cm needle-to-collector distance, a 20 kV applied voltage, and a 1-mL/hour flow rate. Scanning electron microscopy revealed uniform nanofibers with 100 to 250 nm diameters devoid of bead defects. *In-vitro* analysis demonstrated a sustained release profile of azilsartan (AZL), while *in-vivo* studies on rats indicated enhanced wound healing, corroborated by histological examination. The findings suggest that CS/PVA nanofibers, fabricated under these conditions, possess promising characteristics for use as a drug-delivery scaffold in wound treatment applications.

#### INTRODUCTION

Skin is susceptible to injury from various sources, including heat and mechanical forces. [1,2] The therapeutic approach to accelerate healing and reduction of scars entails applying wound dressings to cover injured skin areas. The ideal wound dressing material surpasses its role as a mere physical barrier and creates a microenvironment conducive to exhibiting excellent biocompatibility, creating a moist and adsorbent environment, and excellent scaffold formation. The utilization of materials derived from biological macromolecules has garnered increased attention in this context due to their notable biocompatibility, biodegradability, and renewability. [2,3] Electrospinning is gaining attention for producing nanofibers (NF) with potential therapeutic benefits and

lower toxicity than traditional forms. Using electrostatic force, this technology forms high-viscosity polymer solutions into fibers. Biodegradable/bioresorbable NF scaffolds, particularly for wound dressings, show promise in swift healing, outperforming conventional dressings. Their ECM-like morphology allows customization, drug loading, and prevention of biofilm formation. Nanofibers enhance wound healing through attributes like substantial surface area, moisture control, sustained drug delivery, air exchange, and support for cell processes crucial in tissue regeneration.[4-7] Drug-loaded nanofibers play a pivotal role in various biomedical applications. Dwivedi and colleagues[8] developed modified mats with recombinant human epidermal growth factor and gentamicin to address diabetic wound healing. Similarly, Rathinavel et al.[9] synthesized amine-functionalized

\*Corresponding Author: Ms. Alka

Address: Department of Pharmaceutical Sciences, Babasaheb Bhimrao Ambedkar University (A Central University), Lucknow, Uttar Pradesh, India

**Email** ⊠: alka.psit@gmail.com

Tel.: +91-9453131871

Relevant conflicts of interest/financial disclosures: The authors declare that the research was conducted in the absence of any commercial or financial relationships that could be construed as a potential conflict of interest.

© The Author(s) 2024. **Open Access**. This article is licensed under a Creative Commons Attribution 4.0 International License, which permits use, sharing, adaptation, distribution and reproduction in any medium or format, as long as you give appropriate credit to the original author(s) and the source, provide a link to the Creative Commons licence, and indicate if changes were made. The images or other third party material in this article are included in the article's Creative Commons licence, unless indicated otherwise in a credit line to the material. If material is not included in the article's Creative Commons licence and your intended use is not permitted by statutory regulation or exceeds the permitted use, you will need to obtain permission directly from the copyright holder. To view a copy of this licence, visit <a href="https://creativecommons.org/licenses/by/4.0/">https://creativecommons.org/licenses/by/4.0/</a>

Santa Barbara amorphous (SBA-15) impregnated with curcumin and PVA for wound treatment. Additionally, Ajmal *et al.*,<sup>[10]</sup> formulated ciprofloxacin hydrochloride and quercetin-impregnated PCL-gelatin-based nanofiber dressing material with potent antibacterial and wound healing properties for full-thickness wounds. These electrospun nanofibers offer promising avenues for wound management *via* drug delivery.

The natural polymers have various molecules together in a cluster, resulting in various physical and biological properties such as biodegradation, reduction in inflammation, and bactericidal, fungicidal, and antioxidant properties. It can be used effectively for tissue engineering and various formulations. Chitosan (CS) faces challenges due to inadequate mechanical strength and high adsorption and swelling. [7,11-13] Such challenges are addressed by the integration of CS with various materials for the fabrication of diverse types of wound dressings has emerged as a significant approach. [13, 14] One such material is polyvinyl alcohol (PVA), which exhibits mechanical and biocompatible behavior. As a result, PVA has been found in formulations for tissue repair. Previous studies attempted to combine the benefits of CS and PVA by blending CS with PVA solution to produce composite wound dressing materials.<sup>[7, 13]</sup> Despite these efforts, the resulting materials exhibited suboptimal mechanical properties, biological stability, and durability as wound dressings. [15] Creating an effective electrospinning process requires multifunctional excipients and precise manufacturing steps. Conventional optimization falls short, as it doesn't guarantee the best composition or process. Quality by Design (QbD) using Design of Experiment (DoE) provides a systematic approach, emphasizing understanding and control of both product and process.[1]

Azilsartan, a 2011 USFDA-approved angiotensin II type 1 receptor inhibitor for hypertension, blocks angiotensin II's pressure effects. [16, 17] Besides its anti-hypertensive role, other angiotensin II receptor blockers (ARBs) like losartan and valsartan have shown wound-healing activity. [18] Azilsartan's wound-healing potential, particularly in the literature, remains unexplored. Our study aims to investigate and demonstrate the repurposing of azilsartan medoxomil for wound healing, building on its reported efficacy in periodontitis (a kind of inflammatory condition). In our current investigation, varying proportions of PVA were incorporated to produce nanofiber scaffolds and enhance the properties with CS. The blended nanofiber scaffolds underwent thorough analysis of multiple physical characteristics, including surface morphology and mechanical properties. In this study, azilsartan medoxomil loaded CS/PVA-NF scaffolds were systematically optimized using ObD principles. including risk assessment analysis and response surface methodology, to identify the optimal conditions and composition for scaffold fabrication. Subsequently, the nanofiber scaffolds were comprehensively characterized

through scanning electron microscopy (SEM) for morphological analysis, complemented by *in-vitro* and *in-vivo* experiments aimed at determining their efficacy in tissue repair and regeneration. Considering this, we proposed the fabrication of azilsartan medoxomil-loaded CS/PVA-NF scaffolds.

#### MATERIALS AND METHODS

#### **Materials**

A complimentary sample of azilsartan medoxomil (AZL) was received from CTX Lifesciences, Pvt. Ltd., located in Surat, Gujarat, India. Chitosan (CS), derived from shrimp shells with 75% deacetylation and polyvinyl alcohol (PVA) with 96% hydrolyzation and a typical average molecular weight range of 85,000 to 124,000, was sourced from HiMedia Laboratories Pvt. Ltd. in Mumbai, India.

#### **Animals**

Albino wistar rats (160–200 g) were sourced from LUVAS, Haryana, India, with IAEC approval (Approval Number: BBDNIIT/IAEC/2021/17). Housed in polypropylene cages, they were acclimatized for 7 days under controlled conditions before the study, adhering to ethical guidelines throughout.

#### Methods

Enhancing the quality of nanofiber scaffolds through judicious selection of polymer blend

Chitosan (CS), a polysaccharide obtained from chitin through deacetylation, finds widespread use in biomedical applications due to its remarkable characteristics. These include hydrophilicity, non-toxicity, biocompatibility, biodegradability, antibacterial properties, hemostatic activity, high permeability, and wound-healing capabilities. CS possesses pharmacological attributes that make it highly effective as a wound-healing accelerator. [13, 19]

The nanofibrous scaffolds of CS are particularly fascinating as scaffolding materials, closely resembling cell/tissue components. Researchers have expressed significant interest in a chitosan matrix made of extremely thin fibers, which find diverse uses in cell/tissue regeneration and membrane applications for dressings. However, a notable challenge arises from the difficulty in electrospinning pure CS, primarily due to its solubility exclusively in an acid environment. This solubility causes the NH $_2$  groups in the saccharide backbone to protonate into NH $_3$ , rendering CS positively charged. These positive charges repel each other, resulting in the formation of an uneven bead-like structure. Additionally, the OH and NH $_2$  bonds prevent the formation of smooth fibers, leading to insufficient fiber formation and non-efficient electrospinning. [20]

Two main methods are typically employed to overcome these challenges and achieve continuous thin chitosan fibers. The first method involves blending CS with PVA. The



second method reduces the cationic repulsion between the chitosan fibers with the help of acids such as trifluoracetic acid. However, the latter method is less favored, especially in bio-applications, due to the use of harmful solvents. <sup>[19]</sup> In addressing these issues, the preferred approach is to blend CS with PVA. PVA, being water-soluble, nontoxic, inexpensive, biodegradable, and biocompatible, exhibits excellent electrospinability and forms favorable interactions at the molecular level with CS. This blending with PVA reduces intermolecular interactions between CS molecules, facilitating electrospinning and making it a preferred method for applications such as drug delivery systems.

## Optimizing the final formula and key electrospinning parameters

In this study, our objective was to produce an electrospun scaffold using a CS/PVA base. The fabrication process involved optimizing the final formula and key electrospinning parameters, namely voltage (V), distance from the collection drum to the end of the needle (X), and the rate at which solution is ejected from the needle (Q). Subsequent characterization was conducted stepwise. The process began with determining the optimal formulation of CS and PVA. Then, the optimized formula was applied to assess the optimal conditions. [21, 22] CS/PVA bicomponent electrospun nanofiber scaffolds were produced using a laboratory-scaled electrospinning setup (ES1, E-Spin Nanotech Pvt. Ltd., Kanpur, India).

### Optimizing nanofiber scaffoldS formulations using experimental design methodology

The study aimed to identify a formulation of electrospun CS/PVA-NF scaffolds with desirable radius and adequate physical and biological capabilities. Optimal conditions for minimizing bead formation and achieving the desired nanofiber diameter were determined through a three-factor design. [23]

Key parameters, denoted as V, X, and O, were assessed for formulation optimization. Compositions comprising CS and PVA in a mixture were optimized using varying ratios via the Design of Experiments, with three defined levels of high (+1), medium (0), and low (-1).[23] Based on the findings of the literature, the PVA concentration was determined to be 10 and 12% w/w, while the CS ratio was taken to be 0.5 and 1.5%. Thirteen experimental runs were conducted, and nanofiber producibility, measured on a scale from 1 to 5, served as the response variable. [24] The scale was defined as follows: 1- nanofibers were not formed, only beads were present; 2- very few nanofibers were formed along with beads; 3- uneven thread-like structure; 4- even thread-like structure with very few beads; and 5- uniform nanofibers were formed without any beads, featuring a web-like structure. [25] The software processed the collected responses to formulate an equation and generate graphs depicting the correlation

between the independent and dependent variables, which was able to identify the optimized levels for the fabrication of scaffolds.

#### Preparation of polymeric solution for electrospinning

To prepare the polymeric solution, accurate amounts of CS and PVA were taken as separate solutions of aqueous acetic acid (1% w/v) and deionized water, respectively, serving as the solvent. The concentration of various polymers (CS/PVA) was adjusted according to the experiment's design. The CS solution underwent continuous stirring overnight, while the PVA solution was subjected to  $80^{\circ}$ C,  $700^{\circ}$  rpm, and 6 hours to achieve a uniform mix. This blend was then thoroughly stirred at  $75^{\circ}$ C for the next 2 hours to produce a consistently uniform premix suitable for loading into the syringe for electrospinning. Any unused mixture was stored under refrigeration (4°C) for future use.  $^{[13,15]}$ 

#### Fabrication of nanofiber scaffolds using electrospinning

Each solution underwent a 10-minute sonication period before initiating the electrospinning procedure. Afterward, the premix (5 mL) was taken in a syringe with a needle of 21-G and 4 mm in diameter while maintaining a process temperature of 25°C and ensuring the absence of any bubbles within the solution. A round cylindrical collector (drum), enveloped in aluminum foil, served as the substrate. [20] A systematic exploration of the electrospinning process involved varying three parameters: voltage (ranging from 18–22 kV), flow rate (set between 0.5 to 1.5 mL/h), and nozzle distance (positioned at 7–9 cm) from the collector.

#### Characterization of nanofiber scaffolds morphology

The morphology of the mesh was assessed using advanced microscopic techniques, specifically SEM. Before imaging, suitable gold sputtering was performed on the sample. [26] The ImageJ software (NIH, USA open source) was utilized for processing nanofiber image diameter, expressed as mean  $\pm$  SD. This was done randomly through the images obtained. The diameter in nanometres was plotted with the pattern of frequency (n) where n = 100. Gaussian fitting was employed on the raw data utilizing Origin 2021 software (version 9.8) developed by Origin Lab Corporation to depict anisotropic variation in fiber alignment and the magnitude difference from the mean value. [5, 22]

## Evaluation of physicochemical properties of nanofiber scaffolds

The optimized AZL-loaded nanofiber scaffolds were visually inspected for smoothness. The characterization involves the evaluation of physical appearance, texture, transparency, surface pH, weight variation of nanofiber scaffolds, thickness uniformity, folding endurance, and flatness.

#### • *Physical appearance and texture*

It includes a visual examination of nanofiber scaffolds and an assessment of their texture through tactile examination.<sup>[27]</sup>

#### • Surface pH

The surface pH of nanofiber scaffolds was assessed for possible skin irritation effects. Scaffolds were immersed in 5 mL pH 7.4 phosphate buffer saline (PBS) for swelling. After 15 minutes, the pH was recorded by placing the electrode in contact with the surface of the swollen mesh at room temperature, allowing for a 1-minute equilibration period, and recorded using a digitally calibrated pH meter (Labman LMPH-10 pH meter) in triplicate. [28, 29]

#### • Weight variation test

It was determined to ensure that nanofiber scaffolds contain the appropriate quantity of drug. Five nanofiber meshes from each formulation possessing similar specifications were individually selected and underwent a weight variation test following the procedure outlined in the Indian Pharmacopoeia. Using a digital scale, a portion of film measuring (1.5×1.5) cm<sup>2</sup> was equally cut and weighed to ascertain weight variations. [30] The mean ± standard deviation was computed.

#### • Measurement of thickness

Uniformity of nanofiber mesh thickness is an important parameter affecting almost every free mesh property, viz. permeability, mechanical properties, and folding endurance. Thickness measurements were conducted using a Digimatic outside micrometer (Mitutoyo, Japan). Each nanofiber mesh was placed between the anvil and spindle of the screw gauge, and the digital reading at three different points was recorded for three randomly selected nanofiber meshes to calculate the mean value. [30,31]

#### • Folding endurance

The manual assessment of folding endurance for the optimized nanofiber mesh was conducted in triplicate. A (1.5  $\times$  1.5) cm<sup>2</sup> was cut evenly and folded repetitively at the same location to 180° until fractured or up to 300 folds, indicating favorable nanofiber properties. Folding endurance is a key indicator of mechanical strength, with greater endurance indicating higher strength.<sup>[32]</sup>

#### Flatness

Maintenanin flatness is crucial for nanofiber scaffold integrity. A durability test was conducted on the optimized scaffolds. A longitudinal strips measuring 1.5×0.75 cm were cut from the center and ends. The initial length was recorded before exposure to room temperature for 30 minutes. Any variation in length, indicating non-uniform flatness, was measured to determine the percentage of constriction. Zero percent constriction reflects 100% flatness, calculated using the formula. [33,34]

$$\begin{aligned} \textit{Percentage constriction(\%)} \\ &= \frac{\textit{Initial length of strips} - \textit{Final length of strips}}{\textit{Initial length of strips}} \times 100 \end{aligned}$$

#### Percentage of moisture absorption

The percentage moisture absorption test was conducted to assess the physical stability of nanofiber mesh under highly humid conditions. Initially, the mesh was weighed and then placed in a desiccator with a saturated solution of aluminum chloride, maintaining a relative humidity of  $75 \pm 5\%$  RH at room temperature. After three days, the mesh was removed from the desiccator and re-weighed. [32] The percentage moisture absorption and loss were determined by using a formula.

$$\% \textit{Moisture absorption} = \frac{\textit{Final weight} - \textit{Initial weight}}{\textit{Initial weight}} \times 100$$

#### • Determination of percent drug content

A 1x1 cm² film was accurately weighed, cut into sections, and then placed in a volumetric flask containing 100 mL of PBS with a pH of 7.4. The solution was then subjected to sonication for 20 minutes to ensure uniform drug dissolution, followed by filtration through a 0.45  $\mu$ m pore size membrane to remove any particulate matter. [33] Finally, the absorbance was determined at 248 nm using a UV spectrophotometer.

#### Assessment of drug release profiles and kinetics

The release profiles of AZL-loaded CS/PVA-NF scaffolds were assessed under controlled conditions through in-vitro drug release testing in simulated wound fluid (SWF, pH 7.4) at 37 ± 0.5°C using a Franz diffusion cell setup with separate donor and receptor compartments divided by a dialysis membrane. The release medium (20 mL) was continuously stirred at 100 rpm. Sampling occurred at specified intervals, with medium replacement to maintain sink conditions. Drug release was quantified at 248 nm using UV spectrophotometry, and a calibration curve was employed for drug content determination. [15,35] Data were collected three times and reported as mean ± SD. Drug release mechanisms from nanofiber scaffolds were assessed by fitting release data to zero-order, first-order, Higuchi, and Korsmeyer-Peppas models, with the dominant release kinetic model determined as the one with the highest regression coefficient (r<sup>2</sup>) for the formulations. [15]

#### In-vivo animal studies

In a full-thickness excision wound (FTW) model, [36] the healing properties of AZL-CS/PVA-NF were evaluated. Animals were randomly assigned to five groups: Normal control (NC); full thickness excision wound control (FTW); treated with active pharmaceutical ingredient (AZL); placebo (CS/PVA-NF); and treatment group (AZL-CS/PVA-NF), each with n = 6 animals. Full-thickness wounds were created using sterile biopsy punches, [37-39] and wound dressings, including plain AZL, CS/PVA-NF, and AZL-CS/PVA-NF scaffolds were applied. Pictures of the injured areas were taken on days 1, 3, 7, and 14 postinjury, followed by observation of wound closure for the



subsequent 14 days. Histopathological samples were taken from wound sites post-experiment.

#### Wound closure study

Wound contraction, determined by the percentage reduction in the wound area, served as a metric for treatment effectiveness. Wound healing progress was monitored by covering the wound with a transparent polythene sheet, marking it, and measuring it with a ruler on days 1, 3, 7, and 14. ImageJ software computed wound area from photographs and closure rates were determined using the following equation. [37,38,40]

Wound contraction ratio(WCR)(%)  $= \frac{Area\ of\ original\ wound-Wound\ area\ at\ nth\ day}{Area\ of\ original\ wound} \times 100$ 

#### Histological Analysis Using H and E Staining

Wound biopsies from experimental groups (NC, FTW, and AZL-CS/PVA-NF treated) were collected on days 1, 3, 7, and 14, with a 2-mm skin margin, and fixed overnight in 10% buffered formalin. After dehydration in graded ethanol, tissues were paraffin-embedded. About 5 mm sections were haemotoxylin & eosin (H & E) stained according to established protocols and studied under a digital trinocular microscope for histological evaluation. [37, 38]

#### **Statistical Analysis**

Data underwent further analysis to determine statistical significance, with results presented as mean  $\pm$  SD, measured in triplicate. Statistical analysis utilized GraphPad Prism software (version 8.01), where significance criteria were defined as follows: \*p < 0.05 indicating statistical significance, \*\*p < 0.01 indicating a highly significant level, \*\*\*p < 0.001 indicating a highly significant value, and ns representing non-significant.

#### **RESULTS AND DISCUSSIONS**

## Optimizing The CS: PVA Ratio and Operational Parameters with RSM Analysis

In this research endeavor, the aim was to enhance the electrospinning potential of chitosan by combining it with polyvinyl alcohol and investigating the key electrospinning parameters (voltage, distance, and flow rate) to produce high-quality nanofibers. A total of 13 runs were conducted based on an RSM study, as outlined in Table 1, to assess the nanofiber producibility of different CS and PVA formulations. Subsequently, Table 2 presented 19 distinct conditions for nanofiber production derived from an optimized CS and PVA formula. The equations generated via the experiment's design help establish relationships between ingredient percentages and the respective dependent variable (nanofiber production). These equations were subsequently scrutinized through analysis of variance (ANOVA) as outlined in Table 3, with summarized results presented in Tables 4 and 5. The reliability of the models was evaluated through the *p-value*, with values below 0.05

**Table 1:** CS/PVA concentrations and producibility

Runs	Coded runs		Factors		Response		
	CS	PVA	CS (%w)	PVA (%w)	NF producibility*		
1	0	-1	1.0	10	5		
2	+1	-1	1.5	10	1		
3	-1	+1	0.5	12	4		
4	-1	0	0.5	11	3		
5	-1	-1	0.5	10	2		
6	0	0	1.0	11	2		
7	+1	0	1.5	11	1		
8	+1	+1	1.5	12	1		
9	0	0	1.0	11	3		
10	0	+1	1.0	12	4		
11	0	0	1.0	11	3		
12	0	0	1.0	11	3		
13	0	0	1.0	11	4		

<sup>\*5-</sup> represents uniform nanofibers formed without any beads, featuring a web-like structure, and 1- indicates no nanofibers and only beads.

**Table 2:** DoE for optimization of voltage (V), distance from collection drum to end of needle (X), rate at which solution is ejected from needle (Q)

Runs	Coded runs			Facto	rs		Response		
	V	X	Q	V (kV)	X (cm)	Q (mL/h)	NF producibility* (1-5)		
1	+1	0	0	22	8	1.0	3		
2	-1	+1	+1	18	9	1.5	1		
3	-1	-1	-1	18	7	0.5	1		
4	-1	+1	-1	18	9	0.5	3		
5	+1	+1	-1	22	9	0.5	4		
6	-1	0	0	18	8	1.0	3		
7	0	0	0	20	8	1.0	2		
8	0	0	0	20	8	1.0	1		
9	0	+1	0	20	9	1.0	2		
10	0	0	-1	20	8	0.5	4		
11	-1	-1	+1	18	7	1.5	3		
12	+1	-1	-1	22	7	0.5	4		
13	0	-1	0	20	7	1.0	5		
14	0	0	0	20	8	1.0	1		
15	0	0	0	20	8	1.0	5		
16	+1	+1	+1	22	9	1.5	3		
17	0	0	+1	20	8	1.5	3		
18	0	0	0	20	8	1.0	3		
19	+1	-1	+1	22	7	1.5	1		

<sup>\*5-</sup> represents uniform nanofibers formed without any beads, featuring a web-like structure, and 1- indicates no nanofibers and only beads.

#### Alka and Saraf

Table 3: Analysis of variance (ANOVA) for factors related to the quadratic model

Source	Sum of squares	Degree of freedom	Mean square	F-value	p-value probability >F	•
	Ai	NOVA for diverse CS ar	nd PVA combinatio	ns in nanofiber p	roduction	
Model	15.42	5	3.08	4.42	0.0389	Significant
A-CS	6.00	1	6.00	8.60	0.0220	
B-PVA	0.1667	1	0.1667	0.2388	0.6400	
AB	1.0000	1	1.0000	1.43	0.2702	
A2	8.21	1	8.21	11.76	0.0110	
B2	1.66	1	1.66	2.38	0.1666	
Residual	4.89	7	0.6979			
Lack of Fit	2.89	3	0.9617	1.92	0.2674	Not significan
Pure Error	2.00	4	0.5000			
Correlation total	20.31	12				
	ANG	OVA for diverse electro	spinning paramete	ers in nanofiber p	roducibility	
Model	29.67	9	3.30	6.11	0.0064	Significant
A-V	0.1000	1	0.1000	0.1853	0.6770	
B-X	0.0000	1	0.0000	0.0000	1.0000	
C-Q	0.1000		0.1000	0.1853	0.6770	
AB	6.13	1	6.13	11.35	0.0083	
AC	3.12		3.12	5.79	0.0395	
BC	3.12		3.12	0.0981	0.0395	
A2	0.0529	1	0.0529	9.37	0.7613	
B2	5.06	1	5.06	3.75	0.0135	
C2	2.02		2.02		0.0847	
Residual	4.86	9	0.5398			
Lack of fit	0.8580	5	0.1716	0.1716	0.9599	Not significan
Pure error	4.00	4	0.10000			
Correlation total	34.53	18				

Table 4: The generated equations for ANOVA

Response	The final equation in terms of code factors	p-value	$R^2$	Adj. R <sup>2</sup>	AP
Nanofiber producibility <sup>a</sup>	$3.21-1.00\times A+0.17\times B-0.50\times AB-1.72\times A^2+0.78\times B^2$	0.0313	0.7594	0.5876	6.461
Nanofiber producibility $^b$	3.94+0.1000×A+0.0000×B+0.1000×C+0.8750×AB- 0.6250×AC-0.6250×BC+0.1392×A <sup>2</sup> -1.36×B <sup>2</sup> -0.8608×C <sup>2</sup>	0.0026	0.8593	0.7186	6.373

 $<sup>^</sup>a\mathrm{A:}$  CS, B: PVA.  $^b\mathrm{A:}$  V, B: X, C: Q.

**Table 5:** Appropriate *p-value* for the main parameters

							- P			
	Intercept	cept A		B AB		$A^2$		$B^2$		
Nanofiber producibility <sup>a</sup>	3.2069	-1	0.166667		-0.5		-1.72414		0.775862	
p-values		0.0220	0.6400		0.2702		0.0110		0.1666	
	Intercept	A	В	С	AB	AC	ВС	$A^2$	$B^2$	$C^2$
Nanofiber producibility $^b$	3.93814	0.1	0.63317	0.1	0.875	-0.625	0.625	0.139175	-1.36082	-0.860825
p-values		0.6770	1.0000	0.6770	0.0083	0.0395	0.0395	0.7613	0.0135	0.0847

<sup>&</sup>lt;sup>a</sup>A: CS, B: PVA. <sup>b</sup>A: V, B: X, C: Q.



#### Electrospun Scaffolds for Topical Inflammatory Disease Management

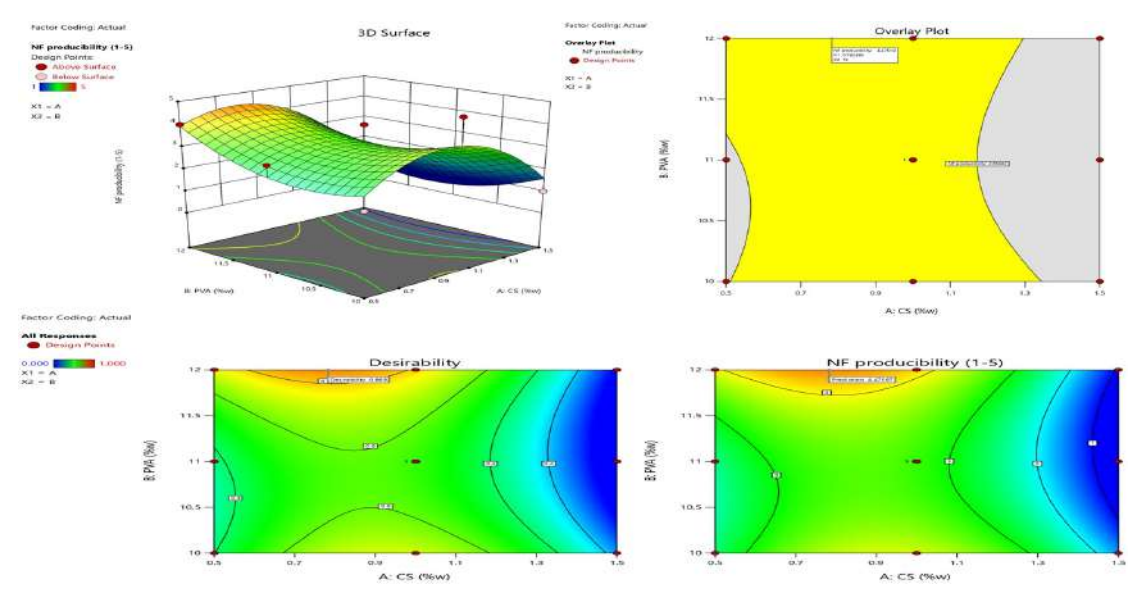


**Fig. 1:** The relationship between the CS/PVA premix effects on the formation of nanofiber. (left) three-dimensional (3D) surface plot and (right) overlay plot (below) contour plot

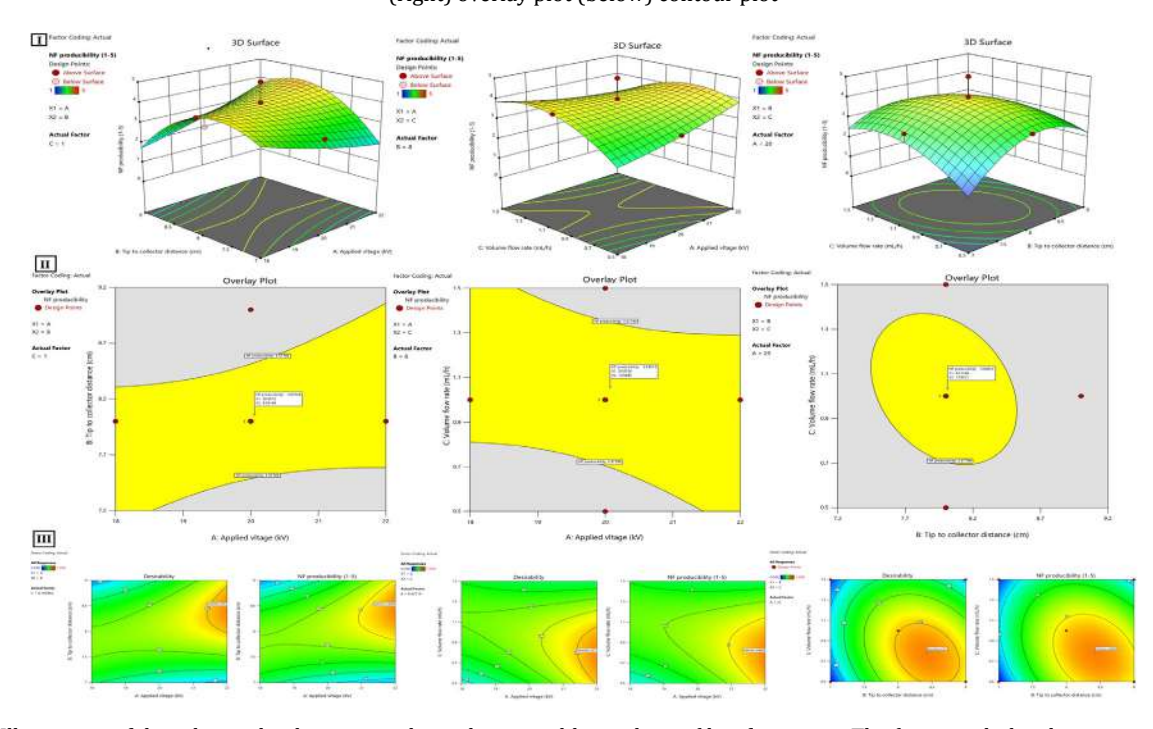


Fig. 2: Illustration of the relationship between independent variables and nanofiber formation. The figure includes three types of plots: (I) a three-dimensional (3D) surface plot, (II) an overlay plot, and (III) a contour plot. Additionally, it mentions that the plots depict the relationships between variables (A) V-X, (B) V-Q, and (C) X-Q

indicating the model's validity and significance. [41] In both studies, *p-values* met this criterion, affirming the models' fitting to the experimental data. Analyzing the impact of CS and PVA percentages on nanofiber production revealed notable effects, especially in the case of the second-order effect of PVA ( $A^2$ ). The models' reliability was further supported by determinant coefficients ( $R^2$ ) and adjusted  $R^2$ , both exceeding 0.50, signifying a satisfactory model fit. [42] Adequate precision (AP) values, exceeding 4 in Table 4, demonstrated a good correlation between values obtained

and theoretical values across various responses. [43].

Fig. 1 depicts the relationship between CS/PVA premix and its corresponding effects on nanofiber production. The contour plots indicated that the optimized ratio of 1% CS and 10% PVA resulted in successful nanofiber production, highlighting the significance of this combination for electrospinning. Subsequent experimentation using the optimized CS: PVA ratio in the main formulation revealed the critical role of process parameters (voltage, distance, and flow rate) in nanofiber quality.

Fig. 2 illustrates these relationships, emphasizing the importance of adjusting these parameters for optimal spinnability. The interplay of voltage (V) and distance (X) revealed that low voltage negatively affected nanofiber production, necessitating a reduction in distance to facilitate spinnability. The relationship between voltage and flow rate (Q) indicated that optimizing Q increased the probability of nanofiber production, with adjustments required as the voltage increased. Examining the effects of flow rate (Q) and distance (X) indicated that an optimal flow rate, approximately 1.0 mL/h, coupled with extended working intervals, significantly enhanced spinnability. In summary, the research underscored the critical role of voltage, distance, and flow rate in optimizing spinnability for the electrospinning process. The findings highlighted the significance of the CS and PVA combination, especially the 1% CS and 10% PVA ratio, in achieving successful nanofiber production. The comprehensive analysis of process parameters provided valuable insights for future advancements in electrospinning technology.

#### **Surface Morphology of Nanofiber Scaffolds**

The production and characterization of nanofiber scaffolds prepared using the electrospinning technique. The scaffolds were optimized by carefully adjusting operational parameters such as polymer concentration, distance from needle to collector, required voltage, and solution ejection rate. [26] SEM analysis revealed that individually prepared nanofibers using CS or PVA exhibited a disordered structure with rough surfaces. However, a significant improvement in structural features was observed when CS (1% w/v) was blended with PVA (10% w/v) at a 1:3 ratio. SEM images showed that the resulting azilsartan medoxomil loaded CS/PVA nanofiber (AZL-CS/PVA-NF) scaffolds had a fine, smooth, and flexible mesh structure with a web-like porous pattern (Fig. 3). The absence

of heterogeneous structures on the nanofiber surfaces (AZL-CS/PVA-NF) suggested thorough dissolution and homogeneous mixing of azilsartan medoxomil with CS/PVA. The mean sizes of the prepared scaffolds (CS/PVA-NF and AZL-CS/PVA-NF) were found to be 119.39  $\pm$  1.1 nm and 224.93  $\pm$  3.02 nm, respectively, demonstrating uniformity along their lengths (Fig. 3).

These dimensions aligned with optimal values for wound healing and closely resembled the extracellular matrix (ECM) of the skin. [45, 46] The fine mesh structure provided a substantial surface area, promoting cell respiration, oxygen supply, and moisture retention—critical factors for expediting wound healing. [47] In summary, the formulated nanofiber scaffolds demonstrated all the necessary physical properties for effective wound healing.

#### **Effect of Polymer Concentration**

#### Effect of CS

CS solutions below 1% lack adequate material for forming fibrous structures, whereas solutions above 1% become excessively viscous for electrospinning, [48] attributed to robust hydrogen bonding between NH<sub>2</sub> and OH groups. The introduction of PVA mitigates these interactions, facilitating spinnability by decreasing the entanglement threshold of CS chains. This effect is akin to the reduction in CS molecular weight, as observed in previous studies. [49,50]

#### Effect of PVA

The incorporation of PVA into nanofiber scaffolds leads to the development of web-like structures with diverse densities. At a PVA concentration of 10%, the resulting web is sparse and uniformly distributed. Conversely, higher concentrations (11 and 12%) yield denser webs with smaller pores, accompanied by increased fiber fusion, film layering, and aggregation. These intricate web-like

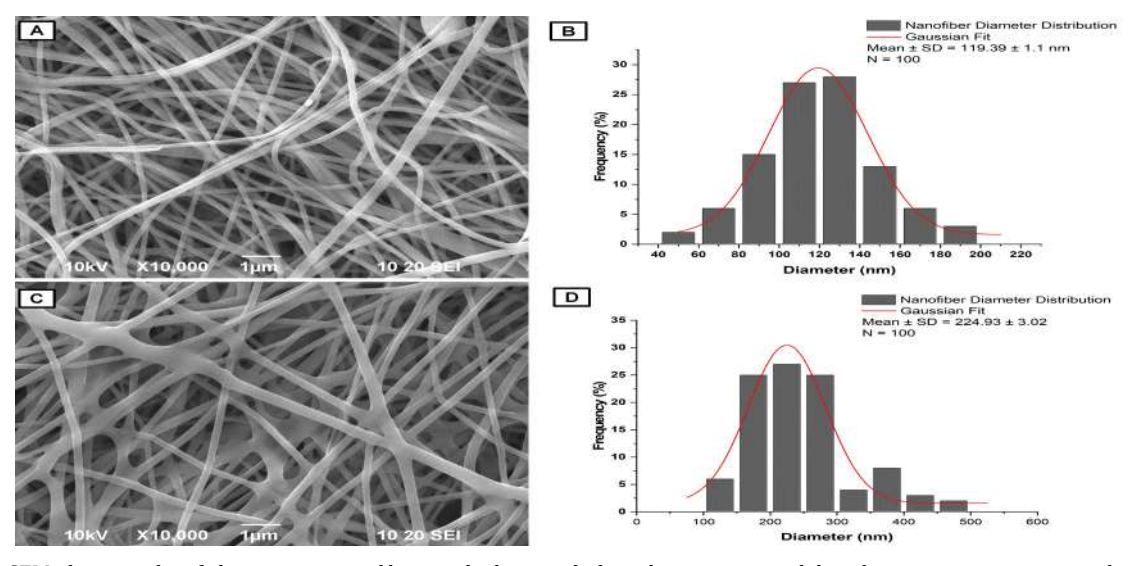


**Fig. 3:** SEM photographs of electrospun nanofiber mesh along with their diameter normal distribution curves, at a magnification of 10,000X: (A, B) for CS/PVA-NF and (C, D) for AZL-CS/PVA-NF



networks bolster scaffold strength, enhancing resistance to deformation. [49, 51] However, in the context of wound dressing applications, the formation of dense mesh-like structures may incur elevated pressure drops, thereby constraining practical usability.

#### Effect of CS/PVA ratio

Precisely controlled conditions are imperative for electrospinning CS due to its inherent positive charges, which repel each other during the process. Although CS solutions exhibit high viscosity, blending with PVA facilitates the fabrication of homogeneous nanofiber scaffolds. Modulating the CS/PVA ratio, such as at 1:3, alters nanofiber morphology, resulting in uniform fibers with a mean diameter of approximately 200 nm. This modification is ascribed to PVA's ability to decrease solution viscosity and disrupt CS's rigid structure. Despite the advantages offered by PVA, CS retains superior properties for drug delivery applications. Consequently, a higher CS/PVA ratio (1:3) proves suitable for electrospun nanofiber scaffold fabrication. [52]

#### Physicochemical Evaluation of AZL-Loaded Nanofiber Scaffolds

#### Physical appearance and surface texture

The optimized AZL-CS/PVA-NF displayed an opaque, uniform, delicate appearance with a smooth texture, observed visually and confirmed by tactile examination. They felt lightweight, flexible, and non-abrasive, indicating a highly porous and breathable structure. Overall, the nanofibers exhibited an aesthetically pleasing appearance and desirable tactile sensation, suggesting their potential suitability for various applications, including wound dressings.

#### Surface pH

For wound healing and skin tissue regrowth, the measured pH should match the pH of the skin. Optimal conditions for fibroblast migration, keratinocyte regeneration, and wound healing were observed within the pH range of 7.2 to  $7.5.^{[53]}$  The surface pH of the optimized AZL-CS/PVA-NF fell within  $7.34 \pm 0.11$ , close to the skin pH in healthy people. The surface pH was almost neutral, minimizing the potential for skin irritation after application.

#### Weight variation test

The optimized AZL-CS/PVA-NF weights were determined to be approximately 21.74  $\pm$  0.15 mg. This indicates consistent weight distribution within the nanofiber scaffolds, suggesting uniformity in fabrication and material dispersion.

#### Thickness uniformity

The optimized AZL-CS/PVA-NF thickness was determined to be approximately  $0.054 \pm 0.01$  mm. The calculated standard deviation values for all cases were small,

indicating consistent film thickness across all samples. This indicates relatively consistent thickness distribution within the nanofiber scaffolds, suggesting uniformity in fabrication and material deposition during the electrospinning process.

#### Folding endurance

The optimized AZL-CS/PVA-NF exhibited remarkable folding endurance, remaining undamaged despite undergoing over 300 folds and displaying no indications of fracture. This indicates exceptionally high physical strength and durability of the nanofiber scaffolds, making them suitable for various applications requiring repeated bending or folding.

#### **Flatness**

The optimized AZL-CS/PVA-NF exhibited a flatness of approximately 99.86  $\pm$  0.003%, indicating minimal constriction (approximating zero), which suggests that the nanofiber mesh is likely to maintain a smooth surface when applied to the skin.

#### **Percentage of Moisture Absorption**

The percentage of moisture absorption for the optimized AZL-CS/PVA-NF samples intended for wound management was determined to be approximately  $11.86 \pm 0.29\%$  after 24 hours of exposure to a controlled humidity environment. This indicates the nanofibers' capacity to efficiently absorb moisture, facilitating a conducive environment for wound healing by maintaining optimal moisture levels at the wound site.

#### **Percent Drug Content**

The optimized AZL-CS/PVA nanofiber scaffolds exhibited a percent drug content of 98.05 ± 1.44%, indicating a superior drug loading capacity of the formulation, a crucial attribute for nanofibers.

#### AZL In-vitro Release and Kinetics

The AZL-CS/PVA-NF formulation exhibited a significant drug release, with a maximum release of 75.57 ± 3.12% within 24 hours, followed by a deceleration phase, as illustrated in Fig. 4((i). In contrast, AZL-S displayed a notably lower release of 20.10 ± 3.23% over the same duration. The considerable increase in AZL release from the optimized AZL-CS/PVA-NF compared to AZL-S (3.76 times) can be attributed to the presence of the drug within the solution. The release pattern of AZL-CS/PVA-NF revealed a biphasic behavior, with an initial burst release (15–20%) within the first hour, followed by sustained release from the core layers of the fibers due to drug diffusion. This dualphase release mechanism suggests the potential of AZL-CS/ PVA-NF for efficient and prolonged drug delivery, where the initial burst release may rapidly achieve the minimum effective concentration while the sustained release ensures a prolonged therapeutic effect. The controlled release observed with AZL-CS/PVA-NF can be attributed to the

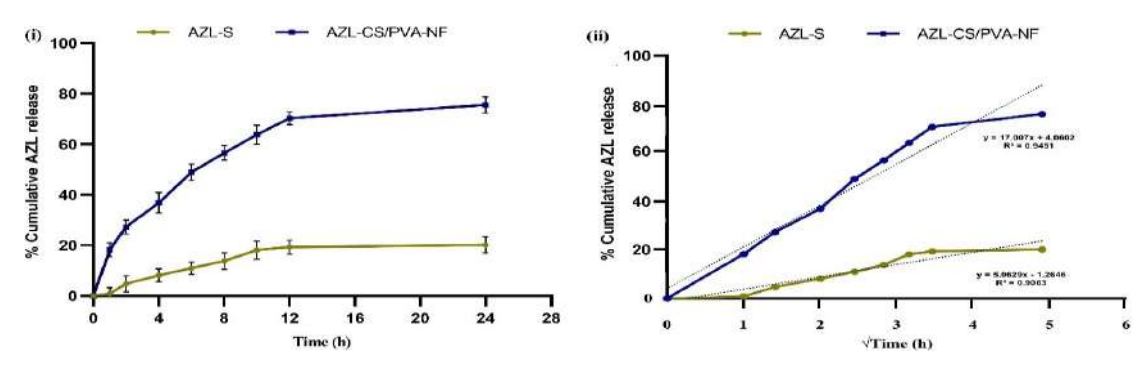


**Fig. 4:** Depiction of two aspects: (i) the AZL release profiles from the nanofiber scaffold compared to the drug diffusion profile from an AZL solution, and (ii) the release profile of AZL-CS/PVA nanofiber, which was well-fitted by the Higuchi model.

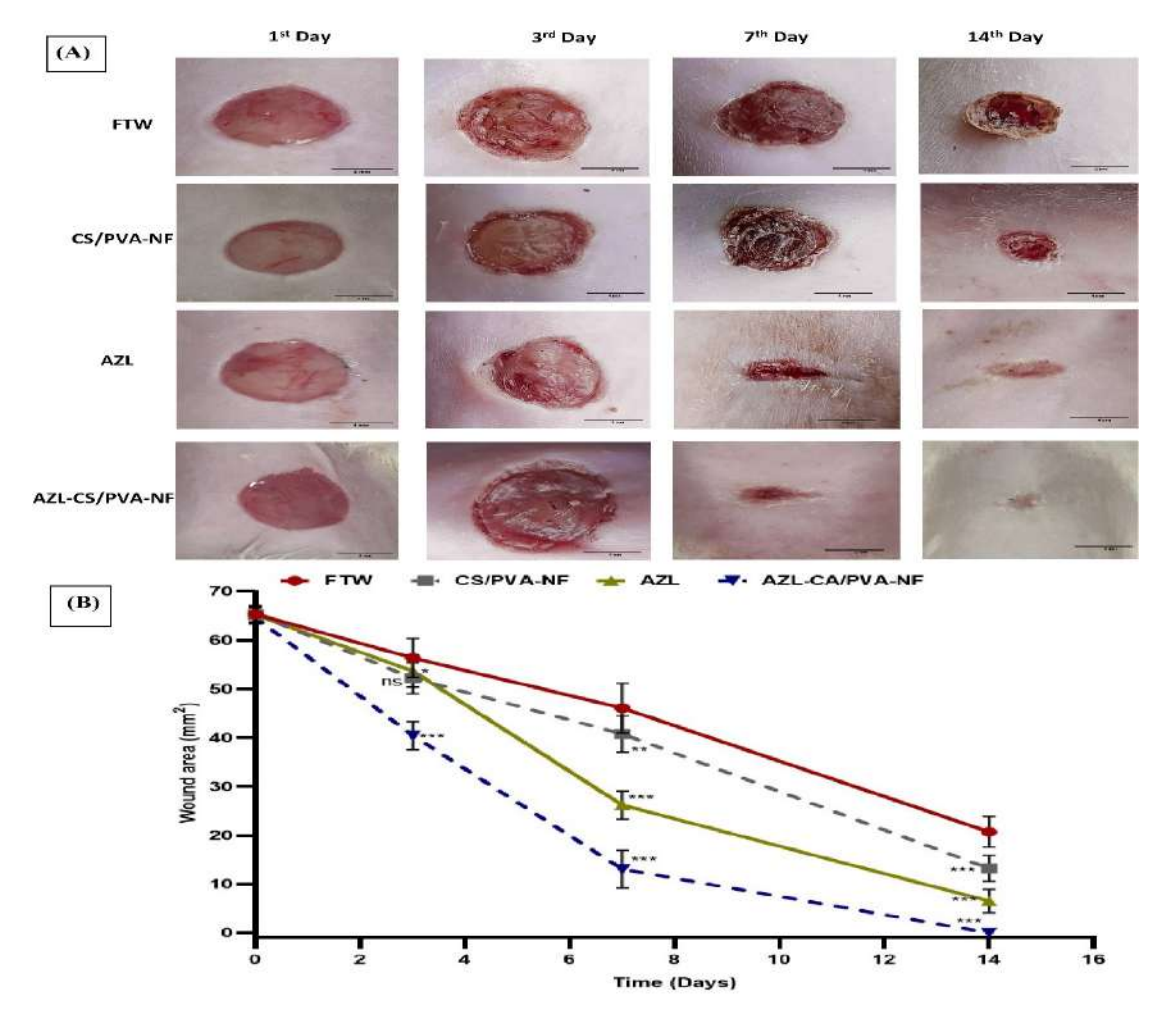


Fig. 5: Visual timeline of wound healing progression across treatment groups. (A) Photographic documentation from days 1, 3, 7, and 14 showcases the evolution of untreated wounds (FTW) alongside those treated with CS/PVA-NF, AZL, and AZL-CS/PVA-NF. Scale bar: 4 mm. (B) Quantified wound closure rates, presented as mean values with standard deviations, offer a comparative evaluation of treatment efficacy over the observation period.

polymers' water-loving nature and rapid swelling rate, facilitating drug release through expanded openings. Additionally, the extensive surface area provided by the fiber mesh network enhances the uniformity of release rates. The improved solubility and dissolution rate of AZL in the formulated AZL-CS/PVA-NF further support its efficacy

compared to the drug solution.[4,54]

The release kinetics of AZL-CS/PVA-NF follow Higuchi kinetics, indicating a synergistic mechanism involving both erosion and diffusion processes within the nanofiber matrix, as evidenced by the high regression coefficient (R<sup>2</sup>) value of 0.9451 (see Fig. 4(ii)).

